TAXONOMY OF STEADY-STATE TWO-PHASE FLOWS IN POROUS MEDIA

Marios S. Valavanides
Dept. of Civil Engineering, University of West Attica, Campus 1, Ag. Spyridonos, Athens, GR-12210, Greece,

This paper was prepared for presentation at the International Symposium of the Society of Core Analysts held in Trondheim, Norway, 27-30 August 2018

ABSTRACT
The phenomenology of steady-state two-phase flows in porous media is recorded in the conventional relative permeability diagrams. A simple Darcy fractional flow analysis, shows that in steady-state conditions the mobility ratio equals the flow rate ratio. Therefore, from every pair of relative permeability measurements we may recover the flow rate ratio, r, and the energy efficiency index of the process, f_{EU}*. The latter expresses a dimensionless measure of the non-wetting phase produced per kW dissipated in pumps.*

A recent, extensive, retrospective examination of relative permeability diagrams [1] identified an important process characteristic, the existence of critical flow conditions (CFC), whereby process efficiency attains locally maximum values. Fractional flow analysis in terms of energy efficiency demonstrate that CFCs define a locus, r(Ca), on the plane of the process' actual independent variables, the capillary number, Ca, and the flow rate ratio, r [2]. To every non-wetting phase /wetting phase /porous medium system, there corresponds a single, unique, CFC locus that can be used as reference locus for characterizing any flow set-up within the same system. The CFC locus lies within a zone delimited by two characteristic r values, whereas the maximum energy efficiency cannot attain a value larger than a specific value that is characteristic of the particular fluid system. By contriving appropriate normative distances of any flow set-up from these characteristic values, it is possible, not only to assess and evaluate the capillary/viscous character of that flow, but also to compare different flows in different systems.*

The procedure described above has been implemented on delivering the so-called "taxonomic coordinates" of many published relative permeability diagrams. Using these coordinates the examined diagrams have been mapped on a two-dimensional, universal, classification map. Sparse or densely populated areas in terms of system properties and flow conditions are revealed.

The proposed methodology is a first attempt towards establishing a systematic classification of relative permeability diagrams pertaining to different flow set-ups in different systems. It may prove useful in building a systematic repository of relative permeability measurements, with scope in better understanding two-phase flows in porous media and/or improving SCAL protocols.

INTRODUCTION
Multi-phase flow in porous media is the process of flow of two or more fluids (liquid

/gas) within a pore network structure. In practice different types of multi-phase flows in porous media may be classified on the basis of various essential characteristics of the associated /examined process. Indicative characteristics -and corresponding classifications- are: time evolution (steady-state, unsteady state), system or mixing characteristics (saturated or unsaturated, two- or- three-phase flow, miscible or immiscible, compressible or incompressible fluids), flow set-up (concurrent, countercurrent, fully developed, non-fully developed), inert or with chemical reaction, etc.

The classification may be of qualitative nature, i.e. it may depend on coarsely defined properties or characteristics across different scales of observation, e.g. connected /disconnected flow, or it can be of quantitative nature, i.e. by evaluating specially /appropriately selected characteristic numbers e.g. capillary number, Bond number etc.

In general, the determination and definition of a characteristic number depends on our understanding of the phenomenon, the system or process that we observe. Typical examples of characteristic numbers in multi-phase flows in porous media are the capillary number or the Bond number. The former compares the magnitude of the viscous forces with the magnitude of the capillary forces. The latter compares the magnitude of the gravity forces to the magnitude of the capillarity induced forces.

In a recent work a methodology was proposed for the normative characterization of steady-state two-phase flow processes [2]. The methodology is based on exploiting the information that is available (or remains in latency) in any steady-state relative permeability diagram. With a simple transformation, from every pair of relative permeability values, it is possible to recover the corresponding values of the flow rate ratio and the energy efficiency of the process -defined as flow rate of non-wetting phase (NWP) per kW of total power dissipated. The latter attains a maximum value that, together with the corresponding value of the flow rate ratio, comprise a uniquely defined pair that can represent the entire data set of the relative permeability diagram. The pair of representative values are compared with nominal, system specific, reference values in order to characterize the conditions that produced the examined relative permeability diagram. Using generalized characteristic numbers, it is possible to compare different processes /systems.

The novelty of the present work relays to implementing the proposed methodology in classifying a total of 180 steady-state runs according to the values of two numbers, the so-called taxonomic coordinates, over a two-dimensional map.

ENERGY EFFICIENCY ANALYSIS OF STEADY-STATE TWO-PHASE FLOWS IN POROUS MEDIA

Consider the simultaneous, one-dimensional concurrent flow of a non-wetting phase (NWP) and a wetting phase (WP) across a porous medium control surface, $\tilde{A}$, at flow rates equal to $\tilde{q}_n$ and $\tilde{q}_w$ respectively. Corresponding pressure differences, are induced upon the two phases. The phenomenological (cause-effect) fractional flow Darcy relations that describe the steady-state, fully developed process are

$$\tilde{U}_i = \frac{\tilde{q}_i}{\tilde{A}} = \frac{\tilde{k}}{\tilde{\mu}_i} k_{ri} \frac{\Delta \tilde{p}}{\Delta \tilde{z}} \quad i = n, w \tag{1}$$

Note that, in the conventional Darcy formulation pertaining to the description of fractional flows, apart from the flow rates and the relative permeabilities, the pressure values are also indexed, $\Delta \tilde{p}_i \quad i = n, w$, to account different pressure values along the NWP and WP. Nevertheless, in steady-state conditions, both phases share a common macroscopic pressure gradient, $(\Delta \tilde{p} / \Delta \tilde{z})$, and the *n/w* indexing may be dropped-out (see Appendix I, eqn (I-2), in [2]).

In general, two-phase flow in pore networks is impeded by a combination of viscous and capillary forces. A relative measure of the viscous over the capillary forces is provided by the value of the capillary number, *Ca*, conventionally defined as

$$Ca = \tilde{\mu}_w \tilde{U}_w / \tilde{\gamma}_{\mathrm{nw}} \tag{2}$$

where $\tilde{\mu}_w$ is the viscosity of the WP and $\tilde{\gamma}_{nw}$ the interfacial tension between the two phases.

The set of superficial velocities may be appropriately reduced and equivalently replaced by a set of dimensionless variables, namely the capillary number, *Ca*, and the N/W flow rate ratio, *r*,

$$r = \frac{\tilde{q}_n}{\tilde{q}_w} = \frac{\tilde{U}_n}{\tilde{U}_w} \tag{3}$$

The reduced rate of mechanical energy dissipation within the process, *W*, can therefore be defined as

$$W = \tilde{W} \, \tilde{k} \tilde{\mu}_w / (\tilde{\gamma}_{\mathrm{nw}} Ca)^2 \tag{4}$$

where, the second term in the product is the inverse of the rate of mechanical energy dissipation of the equivalent -in terms of superficial velocity- one-phase flow of the WP.

The efficiency, $\tilde{e}$, of the process is defined as the ratio of the NWP flow rate, $\tilde{q}_n = \tilde{U}_n \tilde{A}$, over the total mechanical power dissipation, $\tilde{W}$,

$$\tilde{e} = \tilde{q}_n / \tilde{W} \tag{5}$$

Then, by reducing $\tilde{e}$ with the reference energy efficiency $\tilde{e}_{1\Phi}$, of the equivalent one-phase flow of the NWP, the *energy utilization factor*, f_{EU}, can be defined as a dimensionless macroscopic variable, evaluating the energy efficiency of the process in terms of the NWP transport per kW spent in the process,

$$f_{EU}(Ca, r) = \frac{\tilde{e}}{\tilde{e}_{1\Phi}} = \frac{\tilde{U}_n \tilde{W}_{1\Phi}}{\tilde{U}_w \tilde{W}} = \frac{r}{W(Ca, r)} \tag{6}$$

In one dimensional, immiscible, concurrent, steady-state two phase flow in porous media, e.g. in core flows, for each set of measured relative permeability values, $\{k_{rn}(S_w), k_{rw}(S_w)\}$, the corresponding set of flow rate ratio values, *r*, and the energy utilization coefficient, $f_{EU} = r/W$, can be obtained [2] by the transformation,

$$r = \frac{\tilde{q}_n}{\tilde{q}_w} = \frac{\tilde{U}_n}{\tilde{U}_w} = \frac{k_{rn}/\tilde{\mu}_n}{k_{rw}/\tilde{\mu}_w} = \frac{\tilde{\lambda}_n}{\tilde{\lambda}_w} = \frac{1}{\kappa}\frac{k_{rn}}{k_{rw}} \tag{7}$$

and

$$f_{EU} = \frac{k_{rn}}{\kappa(r+1)} = \frac{rk_{rw}}{r+1} = k_{rn}\left(\frac{k_{rn}}{k_{rw}} + \kappa\right)^{-1} \tag{8}$$

where

$$\kappa = \tilde{\mu}_n / \tilde{\mu}_w \tag{9}$$

is the N/W bulk viscosity ratio.

A recent extensive examination of relative permeability diagrams [1], followed by an energy efficiency analysis of the process [2] has identified and proven the existence of *critical flow conditions* (CFCs), i.e. flow conditions $r^*(Ca)$, whereby the energy efficiency of the sought process, eqn (9), takes locally maximum values. A universal map was furnished, illustrating the trends in relative permeabilities and energy efficiency in terms of the capillary number, *Ca*, and flow rate ratio, *r* (Sections 6.1 & 6.2 in [2]). In a follow-up work [3], scaling functions of the flow dependency of relative permeabilities $k_{rn}(Ca, r)$ have been proposed.

According to the findings of these studies, on the high-*Ca* side of the flow regimes, viscosity prevails and the nominal value of the maximum attainable energy efficiency (global maximum or *'ceiling of efficiency')* has been derived considering pure viscous flow conditions ($Ca \to \infty$) as a function of the viscosity ratio, κ,

$$f^*_{EU\infty} = 1/\left(1+\sqrt{\kappa}\right)^2 \tag{10}$$

The corresponding value of the critical flow rate ratio is

$$r^*_\infty = 1/\sqrt{\kappa} \tag{11}$$

On the low-*Ca* side, the critical flow rate ratio, r^*_0, increases because capillarity-related phenomena vis-à-vis the pore network structure are superimposed to viscosity and further impede the flow. Correspondingly, process efficiency drops from a maximum attainable efficiency index (eqn (10)), to zero (due to immobilization of the non-wetting phase). The transition of the CFC locus between these limiting values may be described by an appropriate S-shape function that depends on the physicochemical characteristics of the N/W/PM system [2].

The asymptotic values and the parameters of this S-shape function, provide a unique, effective identification characteristic ('phenotype') of the associated N/W/PM system that may be used as a base reference for comparing and classifying different flow set-ups within different systems. These can be used for the normative characterization of the flow set-up (in terms of viscosity / capillarity) as well as the effective characterization of the pore network (Section 7, [2]).

Note here that, by reducing the variables with equivalent one-phase flow (saturated) variables, the absolute permeability of the porous medium is implicitly taken into account. This is similar to defining unconventional oil reservoirs either as light oil or gas bearing formations of low absolute permeability (tight formations), e.g. light oil- or gas-bearing shales or tight sandstones, or high-viscosity oil bearing formations of high permeability, e.g. heavy oil sands and bituminous sands.

Using the analysis just described it is possible to develop a unified classification based on essential, effective flow characteristics.

COORDINATES OF TAXONOMIC CLASSIFICATION

In regular core analysis, a pair of N/W fluids is continuously injected through a core at different flow rates. When different *i* steady-state conditions settle-in, pressure drops and corresponding flow rates are measured to calculate the set of relative permeability values $\{k_{rn}, k_{rw}\}_i$. These values, together with the corresponding set of measured saturation values $\{S_w\}_i$ are cast into a relative permeability diagram. If the same procedure is repeated at different flow conditions a different rel-perm diagram will be formed -even if the same N/W/PM system is used. This is so because relative permeabilities show a significant dependency on flow rates. One may transform the set of rel-perm data using eqs (7) & (8), and from every *i*-pair of $\{k_{rn}, k_{rw}\}_i$ values compute a pair of $\{r, f_{EU}\}_i$ values. The source and transformed sets of data can be used to cast an extended rel-perm and energy efficiency diagram, similar to the diagrams presented in **Figure 1**.

In all four diagrams of **Figure 1**, red squares and blue triangles sharing the same r_i-abscissas mark pairs of NPW and WP relative permeabilities, $\{k_{rn}, k_{rw}\}_i$. (Source data have been taken from the work of Avraam & Payatakes [4].) Grey circles mark the corresponding energy efficiency values, $\{r, f_{EU}\}_i$, computed using transformation eqs (7) & (8).

In every diagram, the horizontal, dash-dotted red line indicates a nominal value, $f^*_{EU\infty}$, the maximum attainable energy efficiency (the ceiling of efficiency) with that N/W fluid system (when pure viscous flow conditions at very high *Ca* values settle-in); the vertical, dashed red line indicate the corresponding nominal value of the flow rate ratio, r^*_∞.

The four diagrams in **Figure 1** pertain to flow measurements (laboratory runs) using the same glass model pore network. Diagrams on the top and bottom rows [(a)-(b) & (c)-(d)] share N/W fluid systems with the same viscosity ratios, κ; therefore they share in pairs the same nominal values r^*_∞ and $f^*_{EU\infty}$. The left and right column diagrams [(a)-(c) & (b)-(d)] share flow conditions with the same *Ca* values. An extended presentation of similar type diagrams can be found in [1].

From the $\{r, f_{EU}\}_i$ set of each diagram we may detect/select the point corresponding to the maximum value in energy efficiency $f^*_{EU} = \max_i \{f_{EU}\}_i$. We may then measure /compute the logarithmic distance between that maximum and the maximum attainable energy efficiency (the ceiling of efficiency) in that N/W/PM system, $f^*_{EU\infty}$,

$$e^*_\infty = \log\left(f^*_{EU} / f^*_{EU\infty}\right) = \log\left[f^*_{EU}\left(1+\sqrt{\kappa}\right)^2\right] \tag{12}$$

In the same context, we may also measure /compute the logarithmic distance between the corresponding flow rate ratio, r^*, and the nominal value of the flow rate ratio at pure viscous flow conditions (very high values in *Ca*), r^*_∞,

$$d^*_\infty = \log\left(r^*/r^*_\infty\right) = \log\left(r^*\sqrt{\kappa}\right) \qquad (13)$$

The logarithmic distances, d^*_∞, e^*_∞, defining the so-called *taxonomic coordinates* in each relative permeability diagram are clearly indicated in **Figure 1**.

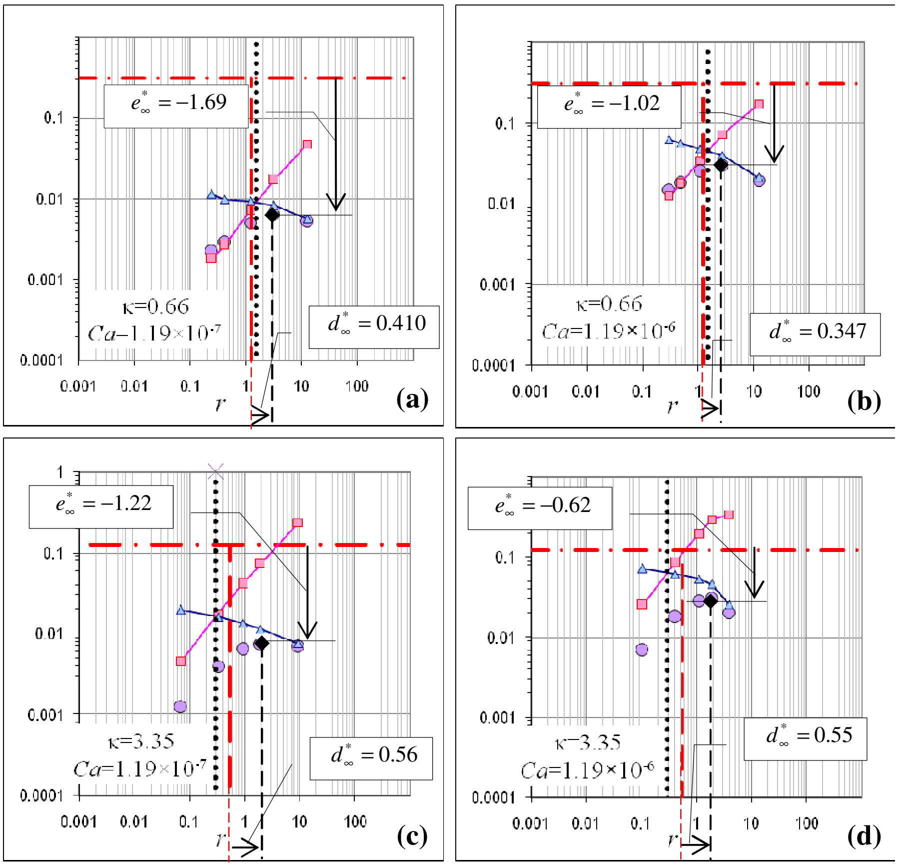

Figure 1 Illustration of the taxonomy coordinates, d^*_∞, e^*_∞, estimated using eqs (13) & (12). □ k_{rn}, △ k_{rw}, ● f_{EU}.

To be able to measure /compute these distances, the maximum energy efficiency value must be detected first, then followed by the detection of the corresponding flow rate ratio. Note, the maximum energy efficiency value cannot always be detected precisely by the available $\{r, f_{EU}\}_i$ set since relative permeability measurements are randomly taken at successive intermediate steps of flow rate adjustments. The finer the partitioning in taking successive steps of rel-perm measurements, the higher the probability of detecting the true local maximum. Good thing is that, because of the structure of the transformation, eqs (7) & (8), the near critical $\left(f^*_{EU}, r^*\right)$ values (approaching the local maximum) can be estimated with great accuracy (see Section 3.2.4 in [1]).

TAXONOMY OF RELATIVE PERMEABILITY DIAGRAMS

The methodology described above has been implemented on mapping ~180 relative permeability data sets and diagrams over a universal, classification map (**Figure 2**).

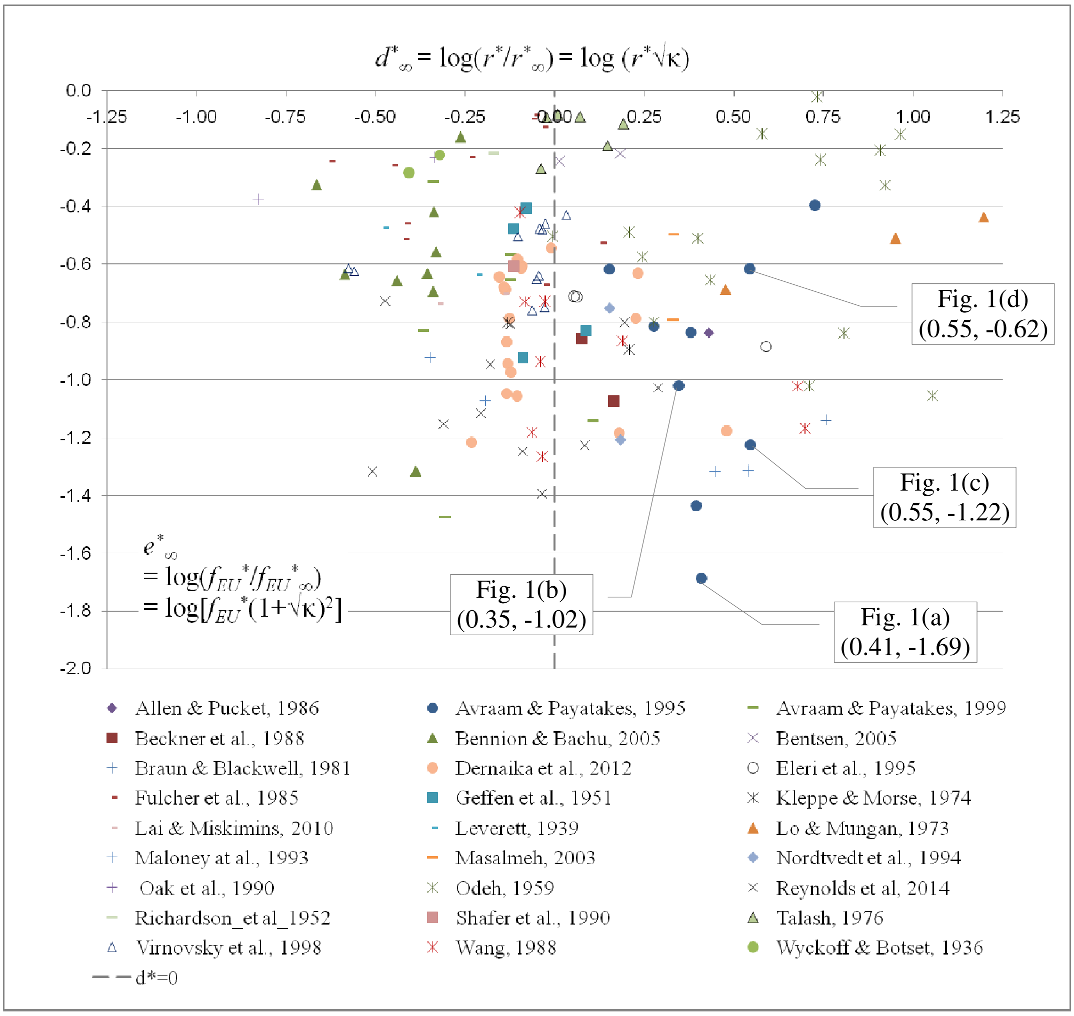

Figure 2 Taxonomy classification of ~180 laboratory runs pertaining to steady-state, two-phase flows in porous media (some of them are virtual runs). Lab runs taken from the same study are indicated with the same marker. Raw data have been taken from [1]. Marked points pertain to diagrams in **Figure 1**.

The source data have been recovered from 35 published laboratory (including a few numerical) studies of steady-state two-phase flow in pore networks, spanning a period of 7 decades. These 179 laboratory runs, pertain to steady-state flows of different pairs of wetting and non-wetting fluids in sand packs, plug cores, glass micro-models and virtual pore network models, including computational fluid dynamics (CFD) or lattice-Boltzmann (LB) simulations (virtual pore network flows), see **Table 1**. The fluids used in the studies were heavy/light oil-brine systems, typical laboratoty fluids (decane /brine), CO_2 etc. Details on the materials and methods used in the relative permeability diagrams, flow conditions and N/W/PM system properties, can be found in [1) & [5]. The report [5] is continuously updated as new diagrams are detected /published and incorporated in this study.

For every relative permeability diagram, the pair of $\{d^*_\infty, e^*_\infty\}$ values is computed and a corresponding point is marked in the 2D classification map (**Figure 2**). Sparsely or densely populated areas of N/W/PM system properties and flow conditions can be detected or delineated. The distribution of markers is indicative and refers only to a part of the entire ecosystem of steady-state relative permeability diagrams.

Table 1 Examined relative permeability diagrams pertaining to a variety of steady-state flows in sand packs, plug cores, glass micro-models and virtual p.m. and fluid systems.

Core plug type	**Lab runs**
Various types consolidated sandstones	74
Loudon, Carbonate, other cores	50
Teflon (consolidated, porous)	3
Propant pack	2
Sandpacks (incl. crushed Pyrex^{TM})	10
Glass pore network models	15
Outcrop chalk	2
Real pore networks subtotal	**156**
Virtual runs (L-B or CFD simulations)	23
In total	**179**

Viscosity ratio, $\kappa = \tilde{\mu}_n / \tilde{\mu}_w$	**Lab runs**
Favorable, $\kappa < 1$	67
$\kappa = 1$	15
Unfavorable, $1 < \kappa$	97
In total	**179**

Constant Ca runs	**82**

CONCLUSION

The phenomenology of two-phase flow in p.m. processes is mainly attributed to the interstitial flow structure, i.e. on the disconnection of the NWP in fluidic elements of varying size and the incessant formation/destruction of numerous N/W menisci. All these phenomena restrain and inhibit -to a certain extent- the superficial transport of NWP and WP. The momentum balance on the entire flow is regulated (a) by the relative intensities of the NWP and WP flows, inducing Stokes flow viscous resistances within the bulk phases, and (b) by the degree of disconnection of the NWP, inducing Young-Laplace capillary resistance across the N/W interfaces separating disconnected NWP from WP and across N/W menisci in contact with the pore walls. Consequently, the rheology of N/W/PM systems shows a strong dependency on flow intensities (superficial velocities).

The proposed methodology is a first attempt towards systematic, orderly classification of relative permeability diagrams pertaining to two-phase flow set-ups within different porous media, based on their presumed natural or *effective* relationships. It can provide deeper understanding of the actual independent variables of the process and opens new possibilities in improving SCAL protocols [2].

The methodology has been implemented on mapping ~180 published relative permeability data sets over a universal, classification map (**Figure 2**), Sparse or densely populated areas of N/W/PM system properties and flow conditions have been revealed.

It can be useful in building a systematic repository of relative permeability measurements, with scope in better understanding two-phase flows in porous media. In that context it may reduce redundancies associated with using non-critical properties to characterize a system, e.g. the absolute permeability of the porous medium is not a critical property when two-phase flow is considered and, as such, it has been amalgamated within the characteristic variables of the equivalent one-phase flow.

The classification is based on the evaluation of two characteristic numbers or taxonomic coordinates, d_{∞}^{*} and e_{∞}^{*}. The classification may be further decomposed and rearranged over a 3D map, by using a third axis to incorporate the effect of the network structure. An example would be to classify relative permeability diagrams according to the extent /intensity of the interaction between wettability (attributed to the physicochemical interaction between the NWP, WP and the pore network solid) and the geometrical structure of the pore network, e.g. classification of carbonates and sandstones or strongly heterogeneous formations, e.g. shales. This of course necessitates the evaluation of characteristic variables describing the pore network structure. In that context, new characteristic numbers need to be introduced /defined (as proposed in Section 7 of [2]). Future research activities should target this problem.

ACKNOWLEDGMENTS

Supported by the Research Council of Norway through its Centres of Excellence funding scheme, project number 262644 is greatly acknowledged.

REFERENCES

1. Valavanides, M.S., Totaj, E., Tsokopoulos, M. (2016) Energy Efficiency Characteristics in Steady-State Relative Permeability Diagrams of Two-Phase Flow in Porous Media *Journal of Petroleum Science & Engineering* **147**, pp. 181-201, doi: 10.1016/j.petrol.2016.04.039
2. Valavanides, M.S. 2018. Review of steady-state two-phase flow in porous media: independent variables, universal energy efficiency map, critical flow conditions, effective characterization of flow and pore network *Transp. in Porous Media*, on-line, 1-55, doi: 10.1007/S11242-018-1026-1
3. Valavanides, M.S., 2018. Universal, True-to-Mechanism, Flow Dependent Relative Permeability Scaling for Steady-State Two-Phase Flow In P.M. *Intern. Symposium of the Society of Core Analysts*, Trondheim, Norway, 27-30/8/2018
4. Avraam, D.G., Payatakes, A.C., 1995. Flow Regimes and Relative Permeabilities during Steady-State Two-Phase Flow in Porous Media. *J. Fluid Mech.* **293**, 207-236, doi: 10.1017/S0022112095001698
5. Valavanides, M.S., Totaj, E., Tsokopoulos, M., 2015. Retrospective examination of relative permeability data on steady-state 2-phase flow in porous media; transformation of rel-perm data (k_{ro}, k_{rw}) into operational efficiency data (f_{EU}). ImproDeProF /Archimedes III, project internal report, http://users.teiath.gr/marval/ArchIII/retrorelperm.pdf